Effect of the Porcine STC-1 Gene on Autophagy and Mitochondrial Function as induced by Serum Starvation

Hao Wang
College of Veterinary Medicine, Yangzhou University/Jiangsu Co-innovation Center for Prevention and Control of Important Animal Infectious Diseases and Zoonosis,

Yuefei Yang
College of Veterinary Medicine, Yangzhou University/Jiangsu Co-innovation Center for Prevention and Control of Important Animal Infectious Diseases and Zoonosis,

Yi Wang
College of Veterinary Medicine, Yangzhou University/Jiangsu Co-innovation Center for Prevention and Control of Important Animal Infectious Diseases and Zoonosis,

Yuehan Peng
College of Veterinary Medicine, Yangzhou University/Jiangsu Co-innovation Center for Prevention and Control of Important Animal Infectious Diseases and Zoonosis,

Yuemin Hu
College of Veterinary Medicine, Yangzhou University/Jiangsu Co-innovation Center for Prevention and Control of Important Animal Infectious Diseases and Zoonosis,

Huiming Ju (hmju@yzu.edu.cn)
College of Veterinary Medicine, Yangzhou University/Jiangsu Co-innovation Center for Prevention and Control of Important Animal Infectious Diseases and Zoonosis,

Lei Xu
College of Veterinary Medicine, Yangzhou University/Jiangsu Co-innovation Center for Prevention and Control of Important Animal Infectious Diseases and Zoonosis,

Research Article

Keywords: STC-1 gene, swine, serum starvation, mitochondria, autophagy

Posted Date: February 17th, 2021

DOI: https://doi.org/10.21203/rs.3.rs-199860/v1

Abstract

Stanniocalcin-1 (STC-1) is a glycoprotein hormone involved in calcium/phosphorus metabolism and direct inhibition of bone and muscle growth. The aim of this study was to investigate the STC-1 gene with respect to the regulatory mechanisms of porcine growth metabolic pathways involving autophagy. PK15 cells were used in this study as control group (CON) cells, and STC-1 gene-knockout PK15 (STC-KO) cells constituted the experimental group. These two groups of cells were subjected to serum starvation to induce autophagy (SCON and SSTC-1 groups). Western blotting was used to detect the expression of autophagy-and mitochondrial function-related proteins, and flow cytometry was used to detect apoptotic cells. Changes in the autophagosome and mitochondrial structure and morphology were observed by electron microscopy. The expression of the autophagy-related proteins LC3B and Parkin was detected by laser scanning confocal microscopy. The results showed that in the CON group and STC-KO group after serum starvation, Pink1 and Parkin expression levels were increased to an extremely high level of significance ($P < 0.01$); LC3B expression was significantly increased ($P < 0.05$); and SQSTM1/P62 expression was increased at an extremely significant level ($P < 0.01$). Electron microscopy revealed that the cells in the serum starvation treatment group all produced autophagosomes. The fluorescence intensity of GFP-LC3B and GFP-Parkin increased significantly ($P<0.05$), indicating that autophagy was successfully induced by serum starvation. After serum starvation, compared to the levels in the CON group, the Bax/Bcl-2 ratio, Pink1 and Parkin protein levels were profoundly reduced in the STC-KO group, at an extremely high level of significance ($P<0.01$). In addition, under serum starvation, the increase in Mfn2, OPA1, and DRP1 proteins was attenuated; the increase in LC3B protein content was significantly attenuated ($P<0.05$); the decrease in LC3B protein content was significantly attenuated ($P<0.05$); the increase in the apoptosis rate was significantly attenuated ($P<0.05$); the decrease in membrane potential was extremely significant ($P<0.01$); the increased amount of active oxygen was significantly attenuated ($P<0.05$); the decrease in ATP was reversed, and this increase was extremely significant ($P<0.01$); the fluorescence intensity of GFP-LC3B was increased; and the increased fluorescence intensity of GFP-Parkin was attenuated significantly ($P<0.05$). These results indicate that autophagy can be caused by serum starvation. Knocking out the porcine STC-1 gene had an obvious-antiapoptotic effect on cells. The inhibition of serum starvation induced autophagy. This is the first study to show that the porcine STC-1 gene confers self-protection in the absence of nutrients, laying the foundation for studying the related mechanism. Knockout cells were used for further study of STC-1 to provide a theoretical basis for studying the effect of STC-1 on pig growth and development.

1. Introduction

STC-1 is a glucocorticoid that was first identified in fish, is released by Steny's microsomes and can inhibit calcium absorption in the gills and intestine, promote phosphate absorption in the kidney and regulate calcium/phosphorus homeostasis1. In mammals, STC-1 is expressed in a variety of tissues, is mainly found in the kidneys and intestines and is an important autocrine and paracrine molecule. Its main function is to influence development by regulating calcium/phosphorus homeostasis and bone

metabolism in vivo, as well as to prevent the normal production of triphosphate adenosine (ATP) by uncoupling proteins in mitochondria 2,3. STC-1 has been found to be a potent active oxygen scavenger in animals. Knocking out STC-1 in animals resulted in an increase in reactive oxygen species (ROS), which affected ROS-mediated biological effects, specifically affecting phosphorylation of certain proteins, increasing superoxide dismutase activity and decreasing caspase-3, P52, IL-6 and interferon-γ expression, thereby increasing anti-inflammatory/antioxidant/anti-apoptotic activity 4,5. Studies have shown that transgenic mice with STC-1 gene overexpression exhibit better disease resistance but have a significantly smaller body size 6,7. Adenosine 5’-monophosphate-activated protein kinase (AMPK) controls energy metabolism by sensing the level of ATP in the cell. It is also called an "energy detector". Studies have shown that STC-1 can promote the expression of utilizable crude protein 2 (UCP2) and Sirtuin 3 (Sirt3) in kidney tissue by activating AMPK. STC-1 expression most likely mediates protein coupling by activating AMPK in certain tissues, such as muscle 8.

Autophagy is a survival mechanism of cells threatened by stress-induced death. Autophagy is induced by a variety of conditions, and amino acids and other small molecules are produced during autophagy because the degraded components of cells can be recycled as building blocks or to produce energy 9. Under starvation conditions, mammalian target of rapamycin (mTOR) is inactivated, and AMPK is activated, which promotes autophagy by catalysing the phosphorylation of serine residues at positions 317, 467, 555, 574, 637 and 777 of ULK110,11. Several studies have shown that an increase in autophagy in a variety of cells can be induced by serum starvation, and in biological organisms, the autophagic process is often initiated under starvation conditions because it helps maintain a the body's internal environment in a steady state12,13. By comparing the expression of the STC-1 gene in different tissues of pigs with different body types, YANG et al. showed that the expression level of STC-1 in Bama mini pigs was significantly higher than that in large white pigs. Bama mini pigs were domesticated from wild pigs in recent years, and they are relatively small and exhibit disease resistance and other characteristics14. Our previous studies on the effects of STC-1 on cell metabolism revealed that changes in STC-1 gene expression levels are closely related to mitochondrial function. A previous study proved that this gene and related signalling pathways are important in maintaining normal mitochondrial function and have been implicated in the development of pig body size. However, the effect of the STC-1 pathway on cell metabolism is unclear, and whether it exerts its biological effects through the autophagic pathway needs to be further investigated. In this study, the authors investigated whether the STC-1 gene has biological effects through the autophagy pathway by measuring cell metabolism and mitochondrial function indicators. By using serum starvation to starve cells and induce autophagy, this study may establish the basis for a deeper understanding of the effects of STC-1 on the growth and development of pigs.

2. Results

2.1 Western blot analysis

The expression of the STC-1 protein was detected by Western blot analysis. GAPDH was the internal control. The relative expression of each target protein was determined by the ratio of the grey value of the target protein band and the grey value of the internal control. The relative expression of the STC-1 protein in the CON group and STC-KO group was 0.47±0.1 and 0.15±0.05, respectively. Compared with that of the Con group, the relative expression of the STC-1 protein in the STC-KO group was lower to extremely significant level ($P<0.01$) (Figure 1).

The western blot analysis of apoptosis-related proteins showed that the ratio of Bax/Bcl-2 in the CON and SCON groups was 0.18±0.01 and 0.4±0.04, respectively. The Bax/Bcl-2 ratios of the STC-KO and SSTC-KO groups were 0.13±0.04 and 0.27±0.03, respectively. After starvation, the ratio of Bax/Bcl-2 in the CON group and STC-KO group increased by 0.22±0.05 and 0.14±0.07, respectively. The increase in the Bax/Bcl-2 ratio in the CON group after serum starvation was significantly higher than that in the STC-KO group after serum starvation ($P<0.01$) (Figure 2).

The western blot analysis of mitochondrial fusion- and fission-related proteins in each group showed that the relative expression levels of Mfn2, OPA1 and DRP1 in the CON group were 0.09±0.04, 0.63±0.13 and 0.22±0.07, respectively. The relative expression levels of Mfn2, OPA1 and DRP1 in the SCON group were 0.19±0.08, 1.59±0.14 and 0.37±0.05, respectively. The relative expression levels of Mfn2, OPA1 and DRP1 in the STC-KO group were 0.14±0.03, 0.34±0.06 and 0.42±0.19, respectively. The relative expression levels of Mfn2, OPA1 and DRP1 in the SSTC-KO group were 0.18±0.1, 0.68±0.11 and 0.48±0.03, respectively. After serum starvation, the relative expression levels of the Mfn2, OPA1, DRP1 proteins increased by 0.1±0.12, 0.96±0.27 and 0.15±0.12 and by 0.04±0.04 and 0.34±0.17 and 0.06±0.22 in the CON group and STC-KO group, respectively. After serum starvation, the protein levels of Mfn2, OPA1, and DRP1 in the CON group were significantly higher than those in the STC-KO group ($P<0.05$) (Figure 3).

The western blot analysis of autophagy proteins showed that the relative expression levels of PTEN induced putative kinase 1(PINK1)and Parkin in the CON and SCON groups were 0.47±0.19 and 0.16±0.02 and 1.76±0.35 and 1.12±0.15, respectively. The relative expression levels of PINK1 and Parkin in the STC-KO group were 0.62±0.18 and 0.11 ±0.02, respectively, and they were 0.83±0.35 and 0.13±0.06 in the SSTC-KO group, respectively. After serum starvation, in the CON group and STC-KO group, the Pink1 and Parkin protein levels increased by 1.29±0.54 and 0.96±0.17 and by 0.21±0.53 and 0.02±0.08, respectively. The increase in Pink1 and Parkin in the STC-KO and SSTC-KO groups was less than the relative expression of Pink1 and Parkin after serum starvation in the CON group ($P<0.01$) (Figure 4).

The relative protein expression level of LC3B in the CON and SCON groups was 0.13±0.01 and 0.21±0.05, respectively. The relative protein expression level of LC3B in the STC-KO and SSTC-KO groups was 0.18±0.03 and 0.2±0.03, respectively. After serum starvation, the relative expression of LC3B protein in the CON group was significantly increased by 0.08±0.06 and 0.02±0.06, respectively, in the STC-KO group. The increase in the relative expression of the LC3B protein after serum starvation in the CON group was significantly higher than that in the STC-KO group after serum starvation ($P<0.05$) (Figure 5).

The relative expression of P62 protein in the CON and SCON groups was 1.43±0.04 and 0.17±0.01, respectively. The relative expression levels of STC-KO and SSTC-KO histones were 0.32±0.03 and 0.13±0.02, respectively. The relative expression of P62 protein in the CON group and STC-KO group after serum starvation decreased by 1.26±0.05 and 0.19±0.05, respectively. The relative expression of P62 protein decreased significantly after serum starvation in the CON group compared with the STC-KO group ($P<0.01$) (Figure 5).

2.2 Cell apoptosis rate analysis

The apoptosis rate of each group was determined by flow cytometry. The results showed that the apoptosis rate of the CON and SCON groups cells was 6.95±0.01% and 13.17±0.03%, respectively. The apoptotic rate of the STC-KO and SSTC-KO group cells was 3.94±0.02% and 5.15±0.02%, respectively. After serum starvation of the CON group and STC-KO group, the apoptosis rate increased by 6.22±0.04% and 1.21±0.04%, respectively. After serum starvation, the apoptosis rate of the STC-KO group cells was significantly lower than that of the CON group cells ($P<0.01$). The apoptotic rate of the CON group and STC-KO cells was significantly increased under autophagy ($P<0.05$), and the apoptosis rate of the STC-KO group cells was significantly decreased ($P<0.05$) (Figure 6).

2.3 Mitochondrial membrane potential analysis

A mitochondrial membrane potential analysis showed that the red-green fluorescence ratio in the CON and SCON groups was 3.15±0.13% and 2.57±0.1%, respectively. The red-green fluorescence ratio of the STC-KO and SSTC-KO groups was 1.44±0.1% and 1.17±0.1%, respectively. The mitochondrial membrane potential decreased by 0.58±0.23% and 0.27±0.2% after serum starvation in the CON group and STC-KO group, respectively. The reduction in cell mitochondrial membrane potential in the STC-KO after serum starvation group was significantly lower than that in the CON group after serum starvation ($P<0.01$) (Figure 7).

2.4 Mitochondrial reactive oxygen species (ROS) analysis

Mitochondrial ROS analysis showed that the ROS ratio of the cells in the CON and SCON groups was 40.55±1.75% and 60.28±0.96%, respectively. The ratio of reactive oxygen species in the STC-KO and SSTC-KO groups was 83.35±1.65% and 98.25±3.05%, respectively. The ratio of reactive oxygen species in the CON group and STC-KO group after serum starvation increased by 19.73±2.71% and 14.9±3.7%, respectively. The increase in mitochondrial reactive oxygen species in the STC-KO and SSTC-KO groups was significantly lower than that in the CON and SCON groups ($P<0.05$) (Figure 8).

2.5 ATP analysis

The mitochondrial ATP of the cells was detected by flow cytometry, and the mitochondrial ATP ratios of the CON and SCON groups were 3.4±0.1% and 2.3±0.3%, respectively. The mitochondrial ATP ratios of the STC-KO and SSTC-KO groups were 6.1±0.8% and 3.2±0.1%, respectively. The cell content in the CON group and STC-KO group after serum starvation was reduced by 1.1±0.4% and 2.9±0.9%, respectively. The reduction in ATP in the STC-KO group after serum starvation was significantly higher than that in the CON group after serum starvation ($P<0.01$) (Figure 9).

2.6 The number and morphological changes of cell mitochondria and autophagosomes

The number and morphological changes of mitochondria and autophagosomes in each group of cells were detected by transmission electron microscopy. The results showed that the cells in the CON group exhibited complete cell morphology and structure, intact mitochondrial morphology and structure, and no autophagosome production. In the SCON group, the cell morphological structure of the cells was complete; however, the mitochondria were enlarged and wrinkled with an increased number of cristae, which were blurry, and autophagic vesicles were produced. In the STC-KO group, the cell morphology and structure were also complete; however, the number of mitochondria in the cells was increased, the mitochondria were damaged, and the mitochondrial crest was blurred. In the SSTC-KO group, the morphology and structure of the cells were complete, but the mitochondrial morphology changes varied, with the number of mitochondrial cristae increased and the cristae blurred. Autophagosomes were produced (Figure 10).

2.7 Immunofluorescence analysis

Through the immunofluorescence technique, a confocal laser microscope was used to detect fluorescence changes. The results showed that the fluorescence values of GFP-LC3B and GFP-PRKN (633 nm) (green fluorescent protein) in the CON group were 63.11±0.18 and 73.56±2.7, respectively. The fluorescence values of GFP-LC3B and GFP-PRKN in the SCON group were 77.04±2.26 and 98.78±3.27, respectively. The fluorescence values of GFP-LC3B and GFP-PRKN in the STC-KO group were 63.02±0.25 and 80.98±0.16, respectively. The fluorescence values of GFP-LC3B and GFP-PRKN in the SSTC-KO group were 76.24±0.93 and 86.49±1.68, respectively. The fluorescence intensity of DAPI and MitoTracker red(MTR) decreased after serum starvation in the CON group and STC-KO group, and the fluorescence intensity of GFP-LC3B and GFP-PRKN (633 nm) was extremely and significantly increased ($P<0.01$). The fluorescence intensity of GFP-LC3B increased after serum starvation in the CON group, which was lower than that in the STC-KO group after serum starvation (Figure 11). The increase in GFP-PRKN fluorescence intensity after serum starvation in the CON group was significantly higher than that in the STC-KO group after serum starvation ($P<0.05$) (Figure 12). The results showed that the autophagy-related protein produced after serum starvation in the CON group was significantly higher than that in the STC-KO group after serum starvation ($P<0.05$).

3. Discussion

The porcine STC-1 gene is expressed in multiple tissues, mainly in the kidney and intestine, to regulate calcium/phosphorus homeostasis through autocrine or paracrine pathways15. Studies have shown that the STC-1 gene is closely related to cell growth, metabolism and mitochondrial function, but the specific mechanism of the effect of STC-1 remains unclear 14. Autophagy is a dynamic equilibrium process that clears protein aggregates and damaged organelles through the autophagosome system16. In this study, porcine PK15 cells and STC-KO cells were treated by serum starvation to induce autophagy, and then, the function and role of STC-1 in autophagy and mitochondrial function were determined.

Mitochondria are dynamic organelles that maintain their morphological and numerical equilibrium through fusion and division, which are closely associated with the number of genes and their encoded proteins. The fusogenic gene Mfn2 is located in the outer mitochondrial membrane and is related to the regulation of OPA1 in mitochondria. When Mfn2 is absent, OPA1 is unable to induce mitochondrial fusion, and similarly, when OPA1 is absent, Mfn2 is unable to function as a fusion agent 17,18. When mitochondrial division occurs, the mitochondrial fission-associated protein DRP1 is recalled to the mitochondria. In this study, the mitochondrial intimal fusion protein OPA1, mitochondrial outer membrane fusion protein Mfn2 and mitotic protein DRP1 were measured to determine whether mitochondrial function was impaired after STC-1 knockout and to determine the difference between normal cells and knockout strains under autophagy conditions. This study found that the expression of Mfn2, OPA1, and DRP1 increased in the CON and STC-KO groups after serum starvation. Compared with that in the CON group after serum starvation, the increase in Mfn2, OPA1 and DRP1 in the STC-KO group was significantly reduced after serum starvation. These results indicate that STC-1 gene knockout can stabilize the cell state and maintain mitochondrial autophagy by promoting mitochondrial dynamics and maintaining mitochondrial function. The morphology and structure of mitochondria in each group were observed by transmission electron microscopy. After STC-1 knockout, the number of mitochondria in the cells was increased, the mitochondrial cristae became blurred, and the mitochondria were swollen and shrunken. These results indicate that knocking out the STC-1 gene in PK15 cells can promote the production of mitochondria, but it has a negative impact on the morphology and structure of mitochondria, thereby inhibiting mitochondrial function.

Mitochondria determine the survival and death of cells and maintain the function and activity of cells. These physiological processes are collectively called mitochondrial homeostasis 19. Mitochondrial autophagy is an important regulatory mechanism of mitochondrial homeostasis in eukaryotes, and elaborate regulatory systems are required to maintain this homeostasis. The mechanisms depending on mitochondrial autophagy in mammals include Parkin-dependent and Parkin-independent mechanisms 20,21. In this study, we examined the mechanism of Parkin-dependent mitochondrial autophagy, that is, autophagy mediated by Parkin and the mitochondrial outer membrane protein PINK1, and detected the role of the STC-1 gene in autophagy induced by serum starvation. PINK1 and Parkin are the main

pathogenic proteins of Parkinson's disease and accumulate in damaged mitochondria. Under normal circumstances, PINK1 enters the intramitochondrial cavity through the translocator of the outer mitochondrial membrane (TOM), interacts with the translocator of the inner mitochondrial membrane (TIM), and finally is transferred to the inner mitochondrial membrane. PINK1 is broken down by Presenilin-associated rhomboid-like protease (PARL) on the inner membrane to maintain low expression levels 22,23. Parkin is an E3 ubiquitin ligase that is inhibited under homeostasis. PINK1 is expressed on the surface of dysfunctional mitochondria, where it simultaneously recruits and activates Parkin 24. This study found that the relative protein expression levels of PINK1 and Parkin in the STC-KO group were lower than those in the CON group. However, when these cells were deprived of serum, a greater decrease in PINK1 and Parkin proteins was found after STC-1 knockdown compared to the decrease in the normal cell group. This finding indicates that when the STC-1 gene is knocked out, the cell will activate autophagic flux due to the self-protection mechanism and then promote the occurrence of autophagy. After serum starvation treatment, compared with SCON group cells, SSTC-KO group cells inhibited autophagy. Observation by laser scanning confocal microscopy showed that after STC-1 gene knockout, the Parkin protein in the cells was higher than that in the CON group, while the number of cells in the SSTC-KO group was lower than that in the SCON group. Through electron microscopy, it was observed that when the STC-1 gene was knocked out, the mitochondria in the cells were damaged, promoting the production of autophagy precursors. Cells produce autophagosomes through a self-protection mechanism, thereby inhibiting apoptosis and maintaining homeostasis.

The detection of the autophagy-related protein LC3B is currently the most widely used measure for detecting autophagic flux. The reduction in LC3B-II is related to excessive activation or blockade of autophagic flux. In this study, a significant increase in LC3B expression in the SCON and SSTC-1 cells was detected by GFP-LC3B laser confocal microscopy. The most important truck protein of selective autophagy, P62, is the bridge between LC3B and the substrate for degradation by ubiquitin. The content of P62 increases when autophagic flow is inhibited, and in contrast, the level of P62 decreases when autophagic flow is initiated 25,26. In this study, the decrease in P62 protein in the SCON group was significantly greater than that in the SSTC-KO cell group. This outcome shows that when the STC-1 gene is knocked out, the autophagic flow is accelerated, indicating that knocking out the STC-1 gene can accelerate cell renewal and exert a certain protective influence on mitochondrial damage.

ROS are oxygen-containing active substances that can destroy proteins, lipids, nucleic acids and other biological molecules, thereby damaging cells and tissues. Studies have shown that STC-1 can inhibit the production of ROS and is an effective oxygen scavenger 8. The results of this study found that ROS and ATP levels in the STC-1-knockout group were much higher than those in the normal group, and the number of cells in the serum-starved group was higher than that in the normal group. The membrane potential of the STC-1- knockout group under serum starvation conditions decreased to a greater extent than that of the normal group. These results indicate that apoptosis was inhibited after STC-1 gene knockout, and the apoptosis rate after serum starvation treatment was much lower than that of the normal group after treatment. Bcl-2 protein has a clear anti-apoptotic effect. BAX is a member of the BCL family and an essential proapoptotic factor. BAX binds to heterodimers (BAX/Bcl-2) to inhibit apoptosis;

the smaller the normal BAX/Bcl-2 ratio is, the stronger the antiapoptotic effect. Western blotting was used to detect Bcl-2 and Bax, and it was found that when the expression of Bax increased, the relative expression of the Bcl-2 protein increased to a greater extent in the STC-KO group. These results indicated that STC-1 gene knockout had an antiapoptotic effect. The results of this study once again proved that STC-1 cells have an anti-apoptotic effect on the molecular level and better anti-apoptotic ability after STC-1 knockout under serum starvation conditions.

In general, this is the first time that the effect of STC-1 gene knockout on porcine kidney PK15 cells was examined by serum starvation-induced autophagy. Porcine STC-1 gene knockout has an obvious antiapoptotic effect on cells and can inhibit the autophagy induced by serum starvation to ensure the long-term survival of cells. In this study, the mechanism of autophagy in the cells expressing the porcine STC-1 gene in the absence of nutrients was preliminarily explored, laying the foundation for studying the regulation and application of body functions after the STC-1 gene is knocked out.

4. Materials And Methods

All experiments were completed at the College of Veterinary Medicine, Yangzhou University. Porcine kidney epithelial (PK15) cells were supplied by the Shanghai Cell Bank of China. The porcine STC-1 gene-knockout PK15 cell line was prepared and preserved by experiment in this study. The PK15 cells were used as the control group (CON), and the STC-1 gene-knockout cells were used as the experimental group (STC-KO). The control group of cells under serum starvation conditions is called the SCON group. The experimental group consisted of STC-1 gene-knockout cells under serum starvation conditions and is called the SSTC-KO group.

4.1 Western blot analysis

Researchers extracted the total protein from each group of cells and then performed sodium dodecyl sulfate-polyacrylamide gel electrophoresis (SDS-PAGE electrophoresis). After the proteins were transferred onto membranes, hybridization detection was performed, and the following antibodies were used: anti-STC-1 (1:1000, sc-14346, Santa Cruz, USA), anti-SQSTM1/P62 (1:800, ab233207, Abcam, England), anti-LC3B (1:1000, ab229327, Abcam, England), anti-Parkin (1:1000, ab233434, Abcam, England), anti-Pink1 (1:1000, #6946S, CST, USA), anti-Bcl-2 (1:500, sc-783, Santa Cruz, USA), anti-Bax (1:500, sc-6236, Santa Cruz, USA), anti-OPA1 (1:500, NB110-55290, N0VUS), anti-Drp1 (1:500, sc-21804, Santa, 2000), anti-Mfn2 (1:500, sc-50331, Santa Cruz, USA), anti-glyceraldehyde-3- phosphate (GAPDH) (1:2000, sc-48166, Santa Cruz, USA). The specific experimental methods are described in the literature.

4.2 Flow cytometry

Cells for each test group were collected separately. An Annexin V-FITC apoptosis kit (C1062S, Beyotime, China) and a cell cycle assay kit (C1052, Beyotime, China) were used to determine apoptosis rate and cell

cycle distribution, respectively, by flow cytometry following the kit manufacturer's instructions. In addition the cells in each group were analysed by flow cytometry using JC-1 with a mitochondrial membrane potential kit (C2006, Beyotime, China) according to the manufacturer's instuctions. A reactive oxygen species detection kit (S0033S, Beyotime, China) was used to detect ROS levels in each group of cells.

4.3 ATP Measurement

The cells of each test group were collected, and relative light unit(RLU) was tested with a kit according to the manufacturer's (S0026, Biyuntian, China) and a chemiluminescence analyser (BioTek, Vermont, USA). The concentration of ATP in the sample was calculated according to the prepared standard curve.

4.4. Morphological changes of the mitochondria and autophagosomes were observed by transmission electron microscopy.

The cells from each experimental group were collected and maintained overnight in 2.5% glutaraldehyde at 4 °C. The cells were washed with 0.05 M phosphate buffer four times; fixed with 1% citric acid for 1.5 h; sliced; dehydrated in 30%, 50%, 70%, 80%, 90% and 100% ethanol for 30 min, and stained twice with uranyl acetate and lead citrate. Photographs taken by transmission microscopy enabled the observation of cell morphology and structure, the determination of the number of mitochondria, and the observation of the autophagosome structure.

4.5 Immunofluorescence

The cells from each experimental group were collected and 100 nM Mito-Tracker Red (MTR) probe (C1035, Beyotime, China) was added. Then, the cells were incubated in the dark and fixed with 4% paraformaldehyde, permeated with PBS containing 0.5% Triton X-100 (T8787, Sigma, USA) for 10 min at room temperature, and blocked with 5% foetal bovine serum at room temperature for 30 min. The treated cells were incubated overnight with anti-LC3B antibody (1:500, ab229327, Abcam, England) and anti-Parkin antibody (1:1000, ab233434, Abcam, England) at 4°C. The cells were incubated with fluorescent conjugated secondary antibodies (Alexa Fluor 647) at room temperature for 2 h and 1 mg/mL DAPI was used to stain the nucleus. Using confocal laser imaging analysis, the cells were targeted by a light source with an excitation wavelength of 358 nm, and the LC3B protein and Parkin proteins were targeted by light with a wavelength of 633 nm.

4.6 Statistical analysis

SPSS 20.0 statistical software was used for the statistical analysis of the data, and the calculated information following a normal distribution was expressed using the means ± standard deviation. All experiments were repeated three times with similar results. All graphical analyses were performed using GraphPad Prism software (version 7.04) for Windows. Statistical comparisons were made with two-tailed Student's t tests and one-way ANOVA. The data are presented as the mean ± s.d. Differences were considered significant when $P < 0.05$.

Declarations

Acknowledgements

This work was supported by the National Natural Science Foundation of China (31872323, 31272405)， the Priority Academic Program Development of Jiangsu Higher Education Institutions (PAPD), Jiangsu Co-innovation Center for Prevention.

Author contributions

H.M.J.,H.W. and Y.F.Y. planned the experiments. H.W., Y.F.Y and Y.H.P designed and finished the molecular experiment. H.W., Y.F.Y and L.X. designed and finished the cell experiments. H.W., Y.F.Y. and Y.M.H performed the data analysis. All authors edited the manuscript.

Competing interests

All authors declare that they have no competing financial interests.

References

1. P, L. F., G, F., E, W. B. S. & F, P. S. Hypocalcin from Stannius corpuscles inhibits gill calcium uptake in trout. The American journal of physiology 254 (1988).
2. G.F., W., M., H., C.M., P. & D.H., C. Purification, characterization, and bioassay of teleocalcin, a glycoprotein from salmon corpuscles of Stannius. Wagner G.F.;Hampong M.;Park C.M.;Copp D.H. 63 (1986).
3. P, E. J. et al. The respiratory effects of stanniocalcin-1 (STC-1) on intact mitochondria and cells: STC-1 uncouples oxidative phosphorylation and its actions are modulated by nucleotide triphosphates. Molecular and cellular endocrinology 264 (2007).
4. Liu, D., Shang, H., Liu, Y. & Tikkanen, R. Stanniocalcin-1 Protects a Mouse Model from Renal Ischemia-Reperfusion Injury by Affecting ROS-Mediated Multiple Signaling Pathways. International Journal of Molecular Sciences 17 (2016).

5. Yang, K., Yang, Y., Qi, C. & Ju, H. Effects of porcine STC-1 on cell metabolism and mitochondrial function. Gen Comp Endocrinol 286, 113298, doi:10.1016/j.ygcen.2019.113298 (2020).
6. Huang, L. et al. Overexpression of stanniocalcin-1 inhibits reactive oxygen species and renal ischemia/reperfusion injury in mice. Kidney Int 82, 867-877, doi:10.1038/ki.2012.223 (2012).
7. Jepsen, M. R. et al. Stanniocalcin-2 inhibits mammalian growth by proteolytic inhibition of the insulin-like growth factor axis. J Biol Chem 290, 3430-3439, doi:10.1074/jbc.M114.611665 (2015).
8. Li-Chun, C., Ning-Ning, X. & Shao-Ping, D. Sweetness-induced activation of membrane dipole potential in STC-1 taste cells. Food chemistry 212 (2016).
9. Glick, D., Barth, S. & Macleod, K. F. Autophagy: cellular and molecular mechanisms. J Pathol 221, 3-12, doi:10.1002/path.2697 (2010).
10. Liu T, Yu JN, Liu Y, Kuang WC, Chen H, Wang XY, Wen X, Jiang Y, Qiu XJ.2019. Effect of electroacupuncture serum on expression of myogenic differentiation antigen and autophagyrelated protein Beclin 1 in cultured muscle satellite cells under starvation.Acupuncture Research 44: 799-804.
11. Shen, C., Yan, J., Jiang, L. S. & Dai, L. Y. Autophagy in rat annulus fibrosus cells: evidence and possible implications. Arthritis Res Ther 13, R132, doi:10.1186/ar3443 (2011).
12. Y, W. C., Z, G. X. & Y, L. H. Hypoxia and Serum deprivation protected MiaPaCa-2 cells from KAI1-induced proliferation inhibition through autophagy pathway activation in solid tumors. Clinical & translational oncology : official publication of the Federation of Spanish Oncology Societies and of the National Cancer Institute of Mexico 17 (2015).
13. Zhang, M. H. et al. Human mesenchymal stem cells enhance autophagy of lung carcinoma cells against apoptosis during serum deprivation. Int J Oncol 42, 1390-1398, doi:10.3892/ijo.2013.1810 (2013).
14. Yang KD, Qi CX, Qi YY.2017. Expression and Distribution Difference Analysis of STC-1 Gene in Big and Small Body Shape Pigs. China anmimal husbandry & veterinary medicine 44: 2845-2850.
15. Ryosei, M. et al. Stanniocalcin-1 promotes metastasis in a human breast cancer cell line through activation of PI3K. Clinical & experimental metastasis 31 (2014).
16. Beale, R. et al. A LC3-interacting motif in the influenza A virus M2 protein is required to subvert autophagy and maintain virion stability. Cell Host Microbe 15, 239-247, doi:10.1016/j.chom.2014.01.006 (2014).
17. Ana, N., Carmen, G., M, L.-C. J. & Alberto, B. Beneficial effects of moderate exercise on mice aging: survival, behavior, oxidative stress, and mitochondrial electron transfer. American journal of physiology. Regulatory, integrative and comparative physiology 286 (2004).
18. Ding, W. X. et al. Autophagy Reduces Acute Ethanol-Induced Hepatotoxicity and Steatosis in Mice. Gastroenterology 139 (2010).
19. Alsayyah, C., Ozturk, O., Cavell ini, L., Belgareh-Touzé, N. & Cohen, M. M. The regulation of mitochondrial homeostasis by the ubiquitin proteasome system. BBA - Bioenergetics 1861 (2020).

20. Liu, L., Sakakibara, K., Chen, Q. & Okamoto, K. Receptor-mediated mitophagy in yeast and mammalian systems. Cell Res 24, 787-795, doi:10.1038/cr.2014.75 (2014).
21. Springer, M. Z. & Macleod, K. F. In Brief: Mitophagy: mechanisms and role in human disease. Journal of Pathology 240, 253-255, doi:10.1002/path.4774 (2016).
22. Klein, C. & Westenberger, A. Genetics of Parkinson's disease. Cold Spring Harb Perspect Med 2, a008888, doi:10.1101/cshperspect.a008888 (2012).
23. Meissner, C., Lorenz, H., Weihofen, A., Selkoe, D. J. & Lemberg, M. K. The mitochondrial intramembrane protease PARL cleaves human Pink1 to regulate Pink1 trafficking. J Neurochem 117, 856-867, doi:10.1111/j.1471-4159.2011.07253.x (2011).
24. Nguyen, T. N., Padman, B. S. & Lazarou, M. Deciphering the Molecular Signals of PINK1/Parkin Mitophagy. Trends Cell Biol 26, 733-744, doi:10.1016/j.tcb.2016.05.008 (2016).
25. Kwon, Y. T. & Ciechanover, A. The Ubiquitin Code in the Ubiquitin-Proteasome System and Autophagy. Trends Biochem Sci 42, 873-886, doi:10.1016/j.tibs.2017.09.002 (2017).
26. Seok, K. J. et al. Prognostic Significance of LC3B and p62/SQSTM1 Expression in Gastric Adenocarcinoma. Anticancer research 39 (2019).

Figures

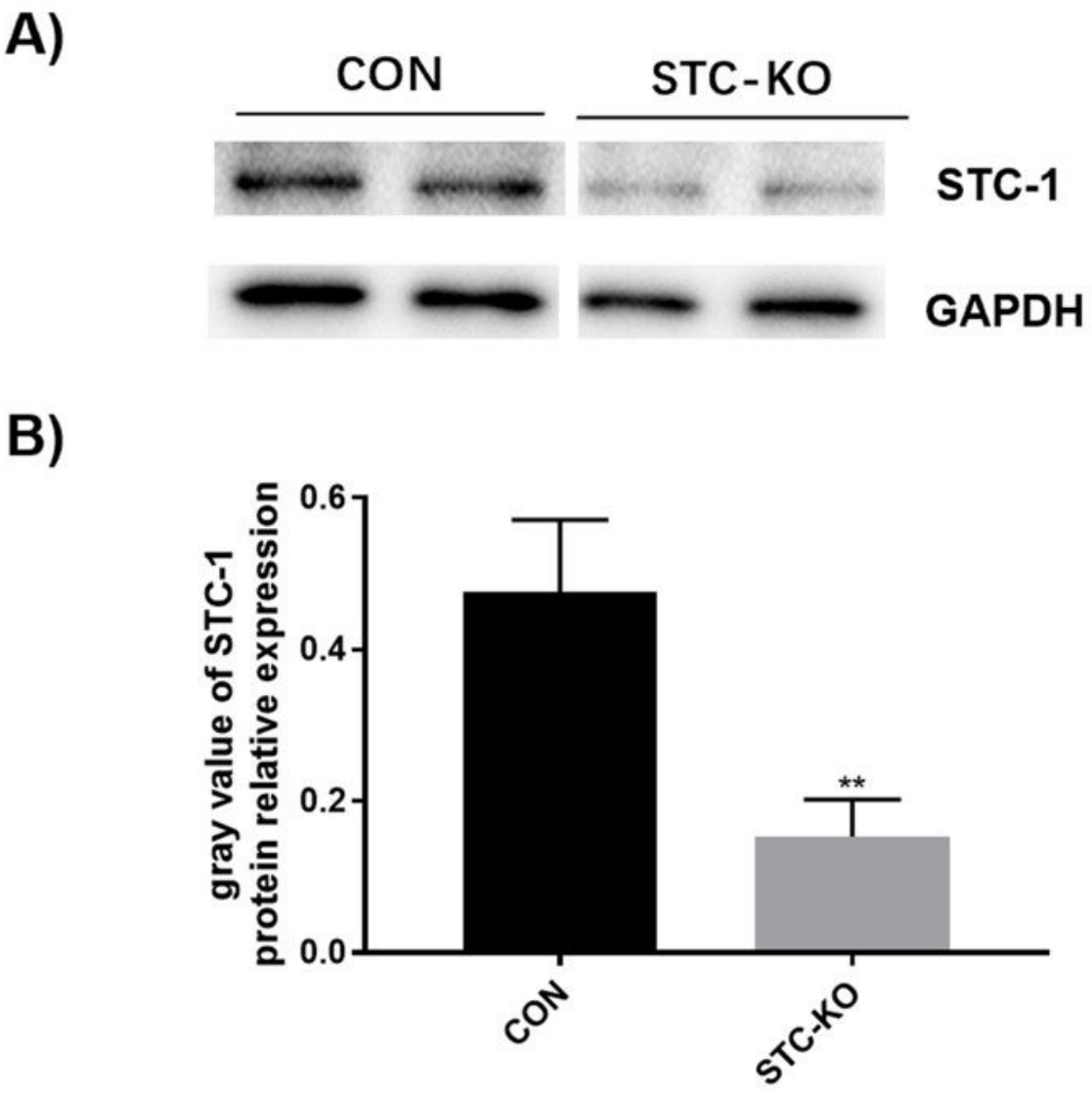

Figure 1

Western blotting was used to detect the relative expression of the STC-1 protein in PK15 cells. A) Western blot hybridization detection of STC-1 and GAPDH. B) Grey analysis of the relative expression of each cell protein on STC-1 cells. Statistical comparisons were made with two-tailed Student's t tests, and one-way ANOVA. The data are presented as the means ± s.d. (n=3). Changes were considered statistically significant when $P < 0.05$ and $P<0.01$.

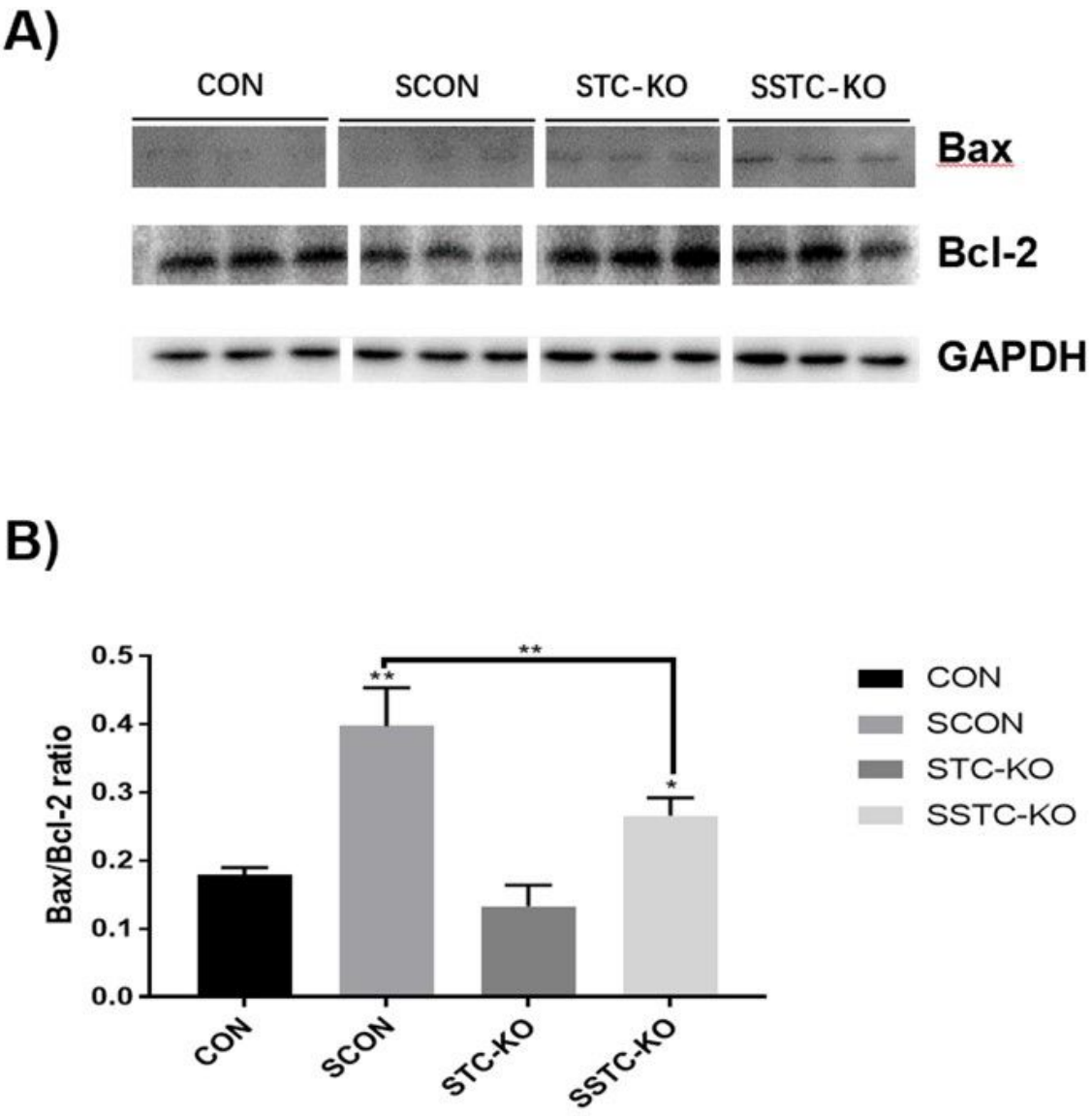

Figure 2

Western blot detection of the expressed apoptotic proteins in PK15 cells. A) The results from the Western blot analysis. B) Grey analysis of the relative expression of each cell protein on BAX/BCL-2 cells. Statistical comparisons were made with two-tailed Student's t tests, and one-way ANOVA. The data are presented as the means ± s.d. (n=3). Changes were considered statistically significant when $P < 0.05$ and $P<0.01$.

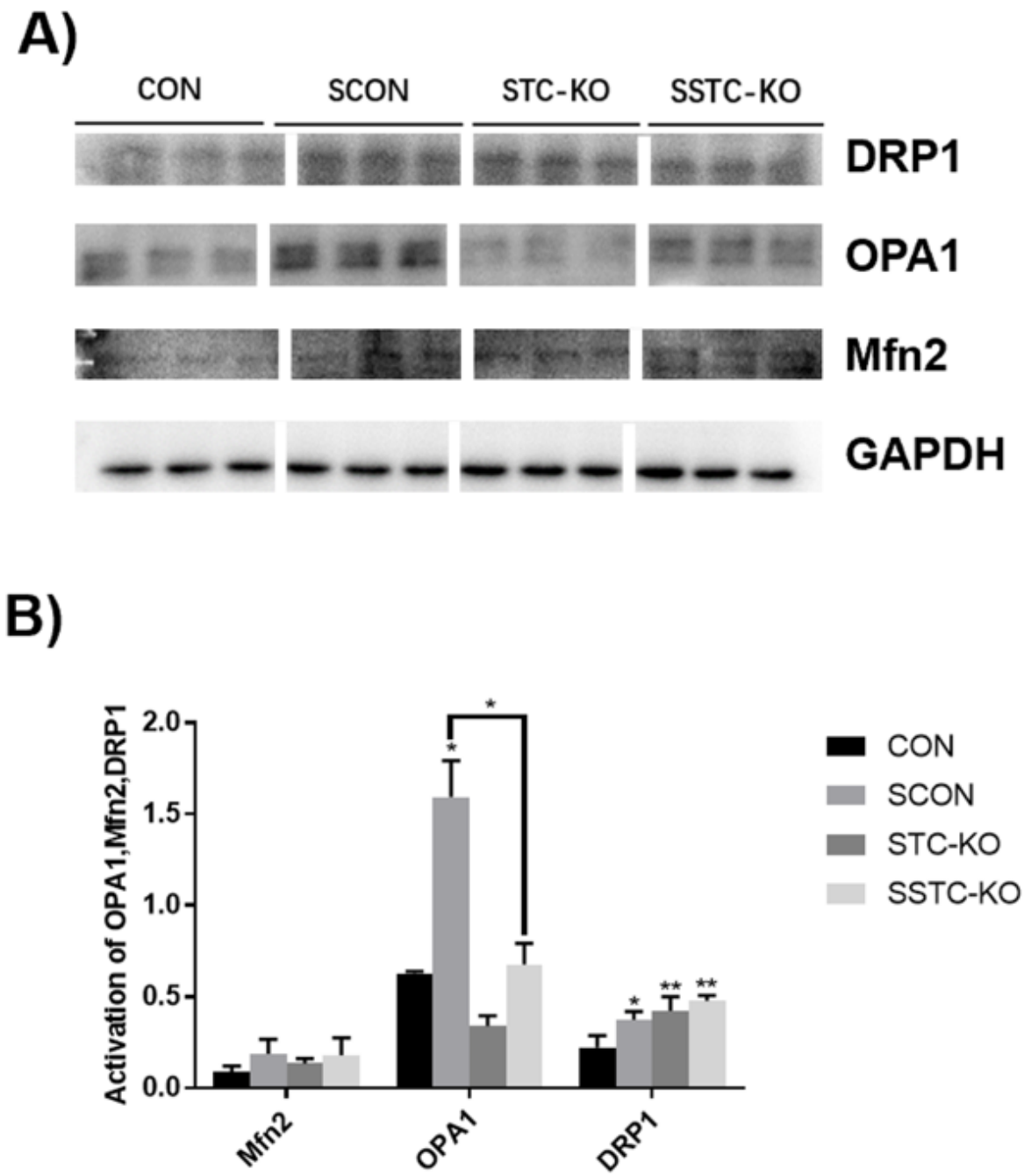

Figure 3

Western blotting was used to detect the intracellular STC-1 and relative mitochondrial-related protein expression levels. A) The results from the Western blot analysis. B) Grey analysis of the relative expression of each cell protein on DRP1, OPA1, and Mfn2 levels. Statistical comparisons were made with two-tailed Student's t tests, and one-way ANOVA. The data are presented as the means ± s.d. (n=3). Changes were considered statistically significant when $P < 0.05$ and $P<0.01$.

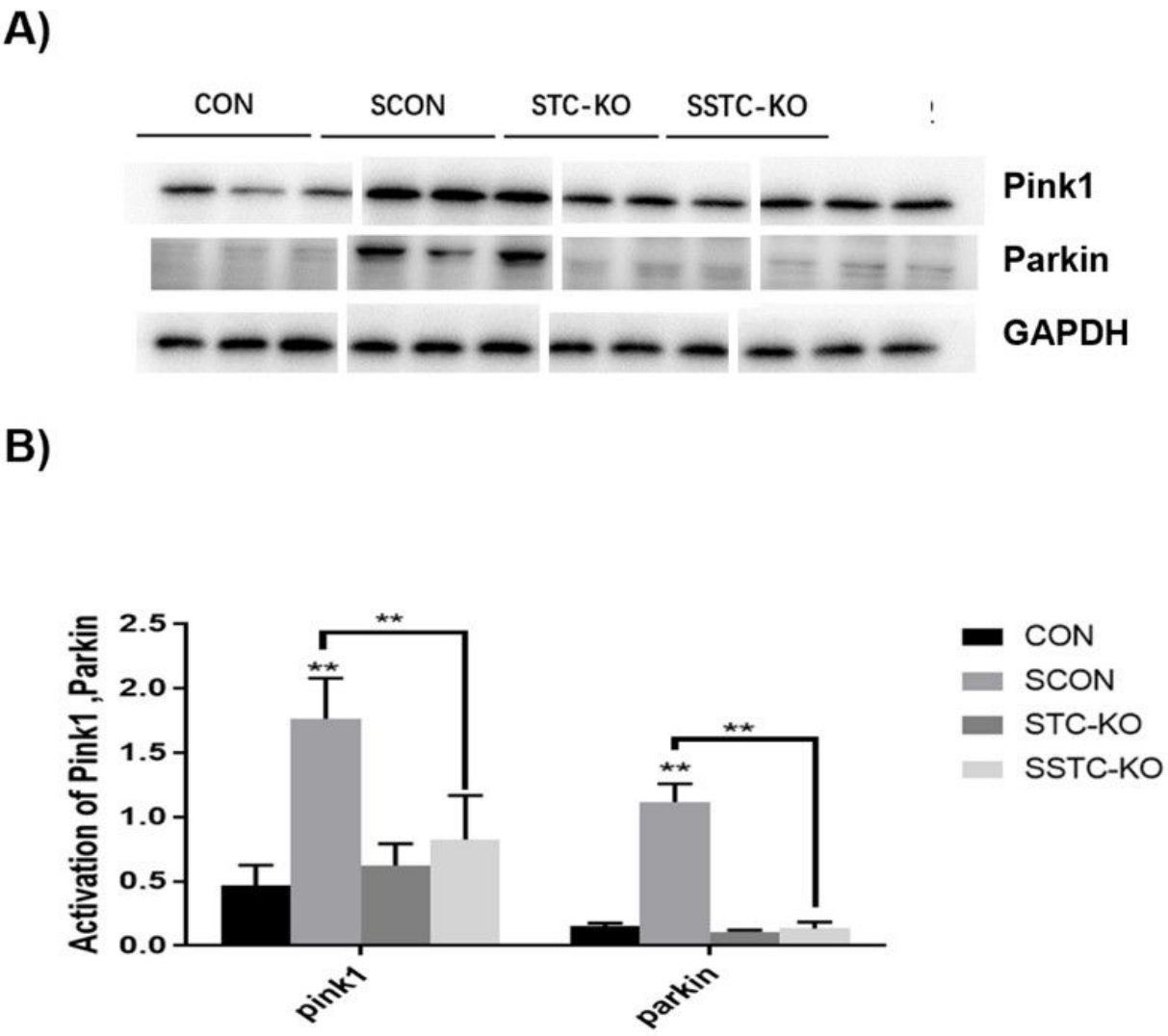

Figure 4

Western blot detection of the expressed autophagy proteins in PK15 cells. A) The results from the Western blot analysis. B) Grey analysis of the relative expression of each cell protein relative to that of pink1 and Parkin. Statistical comparisons were made with two-tailed Student's t tests, and one-way ANOVA. The data are presented as the means ± s.d. (n=3). Changes were considered statistically significant when $P < 0.05$ and $P<0.01$.

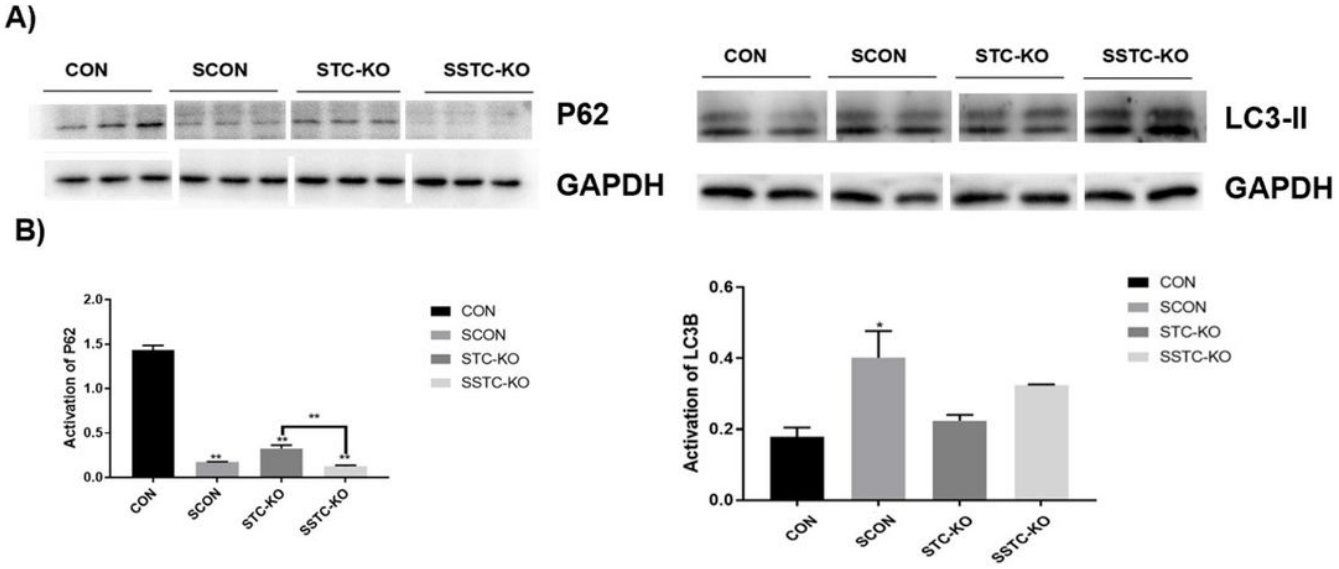

Figure 5

Western blot detection of the expressed autophagy proteins in PK15 cells. A) The results from the Western blot analysis. B) Grey analysis of the relative expression of each cell protein relative to that of on P62 and LC3II. Statistical comparisons were made with two-tailed Student's t tests, and one-way ANOVA. The data are presented as the means ± s.d. (n=3). Changes were considered statistically significant when $P < 0.05$ and $P<0.01$.

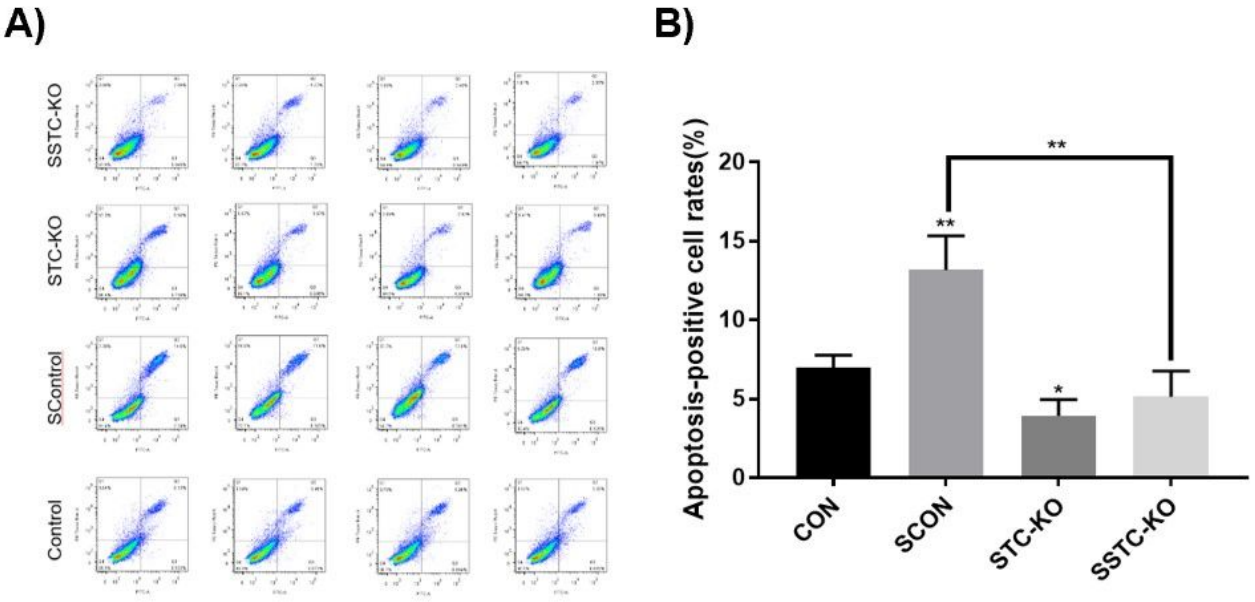

Figure 6

Flow cytometry to detect the apoptosis rate. A) Flow cytometry results. B) Analysis of the apoptosis rate of the SCON, STC-KO, SSTC-KO and CON groups. Statistical comparisons were made with two-tailed Student's t tests, and one-way ANOVA. The data are presented as the means ± s.d. (n=3). Changes were considered statistically significant when $P < 0.05$ and $P<0.01$.

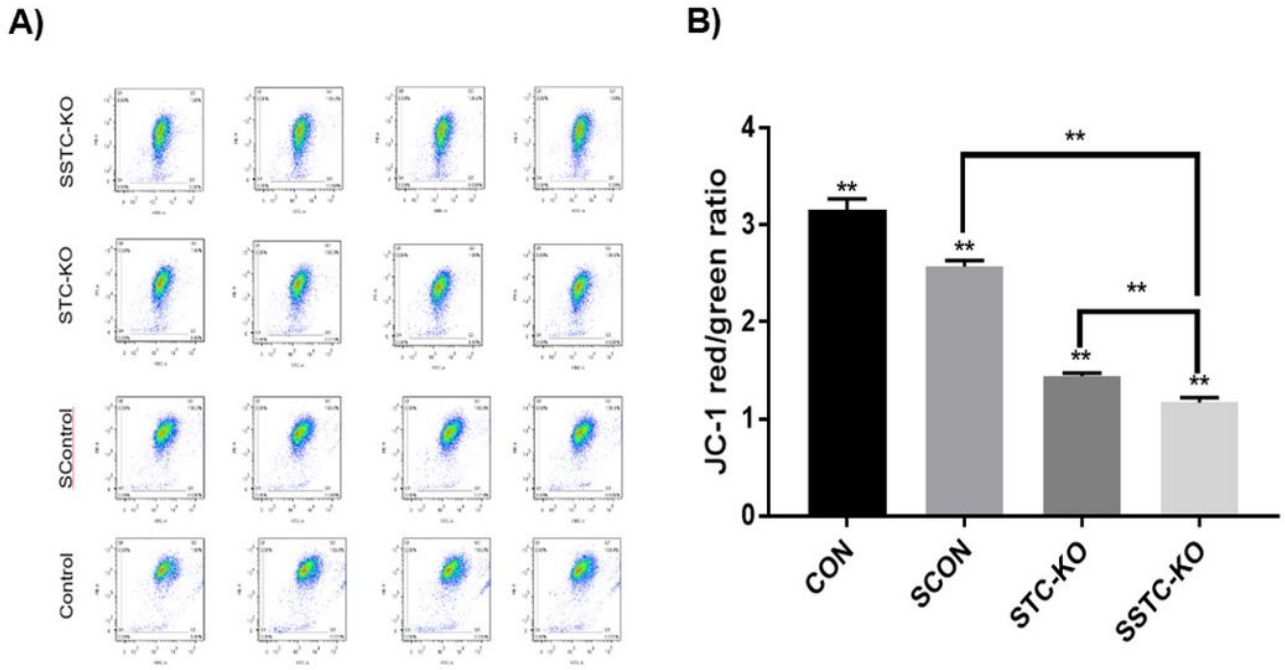

Figure 7

Flow cytometry was used to detect and analyse the membrane potential of each group. A) Flow cytometry results. B) Analysis of the membrane potential of the SCON, STC-KO, SSTC-KO and CON groups. Statistical comparisons were made with two-tailed Student's t tests, and one-way ANOVA. The data are presented as the means ± s.d. (n=3). Changes were considered statistically significant when $P < 0.05$ and $P<0.01$.

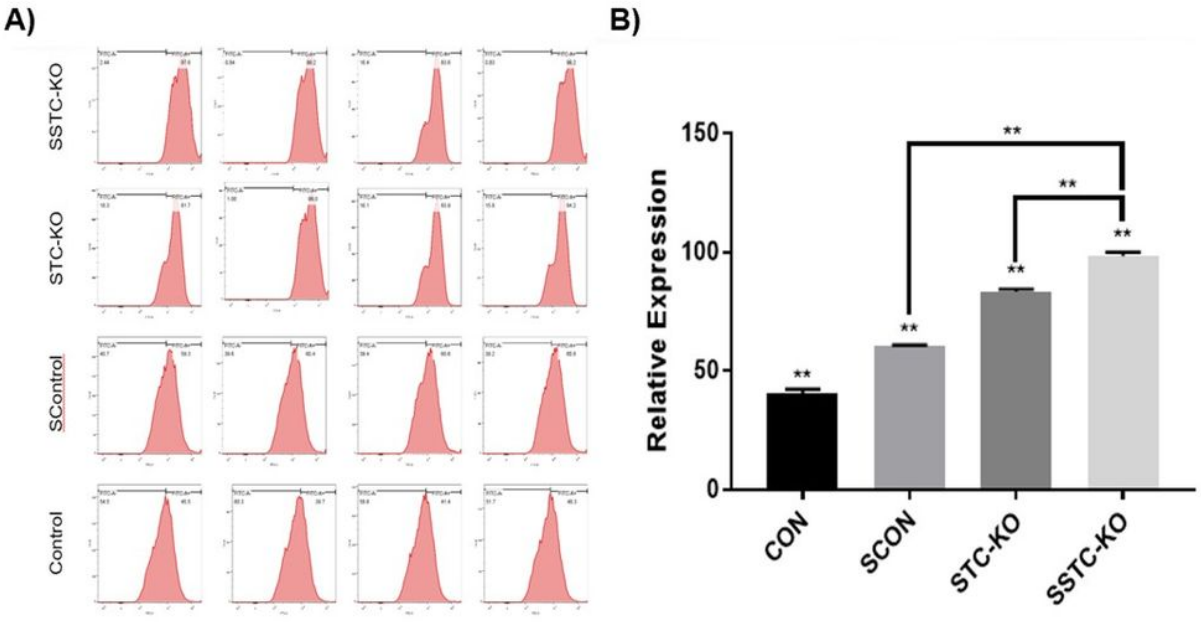

Figure 8

Flow cytometry detection and analysis of mitochondrial reactive oxygen species in each group of cells. A) Flow cytometry results. B) Analysis of the reactive oxygen species in the SCON, STC-KO, SSTC-KO and CON groups. Statistical comparisons were made with two-tailed Student's t tests, and one-way ANOVA. The data are presented as the means ± s.d. (n=3). Changes were considered statistically significant when $P < 0.05$ and $P<0.01$.

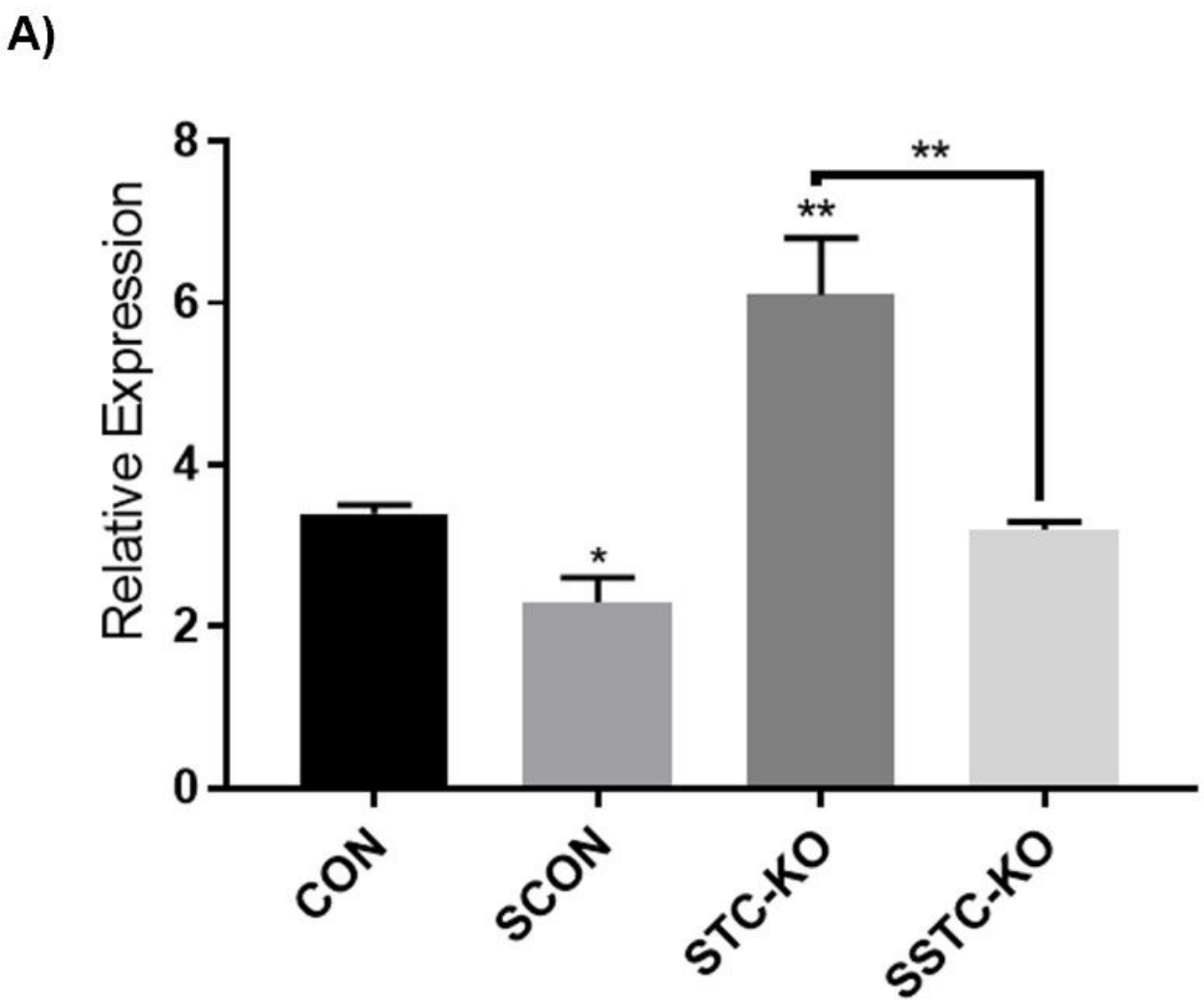

Figure 9

Mitochondrial ATP detection.

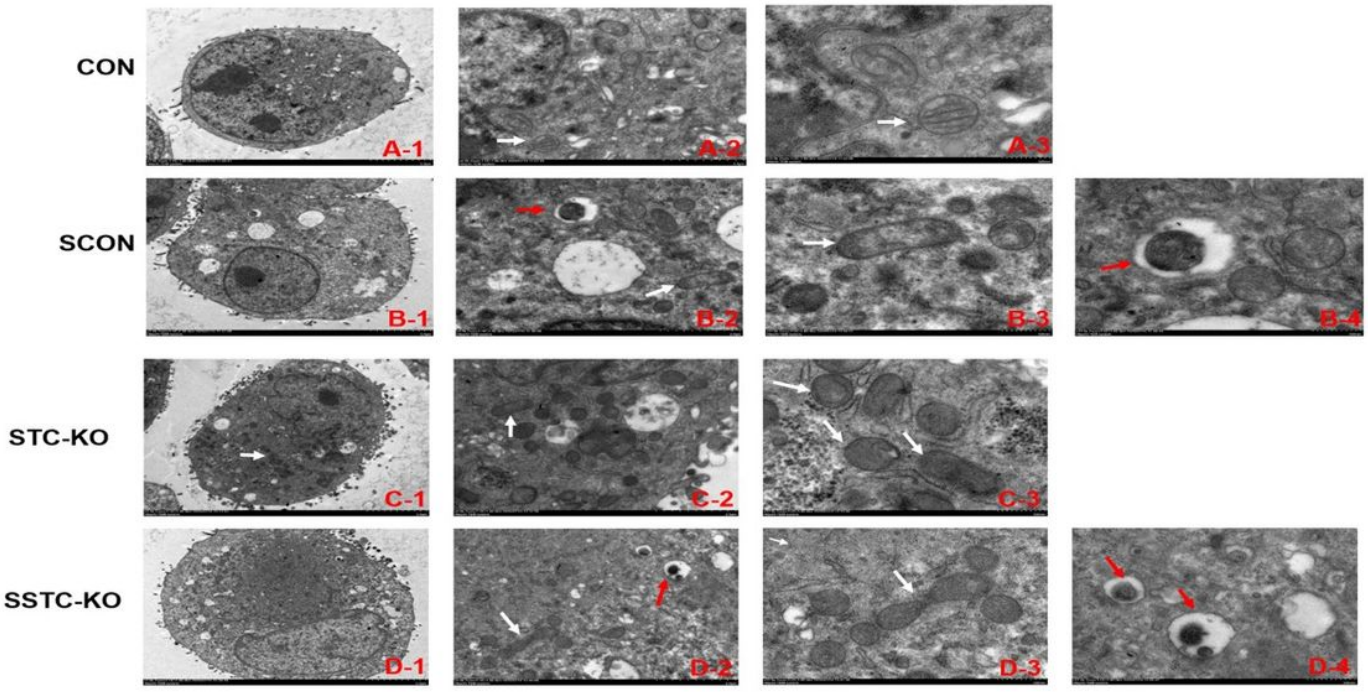

Figure 10

Morphological changes in mitochondria in PK15 cells were observed by transmission electron microscopy. In these cells, we assessed the integrity of the cell membrane, the structural position of the nucleus and the structure of mitochondria (white arrow), and the formation of autophagosomes (red arrow). Scale bars: 1) 5.0 μm, 2) 2.0 μm, and 3) and 4) 500 nm. Statistical comparisons were made with two-tailed Student's t tests, and one-way ANOVA. The data are presented as the means ± s.d. (n=3). Changes were considered statistically significant when $P < 0.05$ and $P<0.01$.

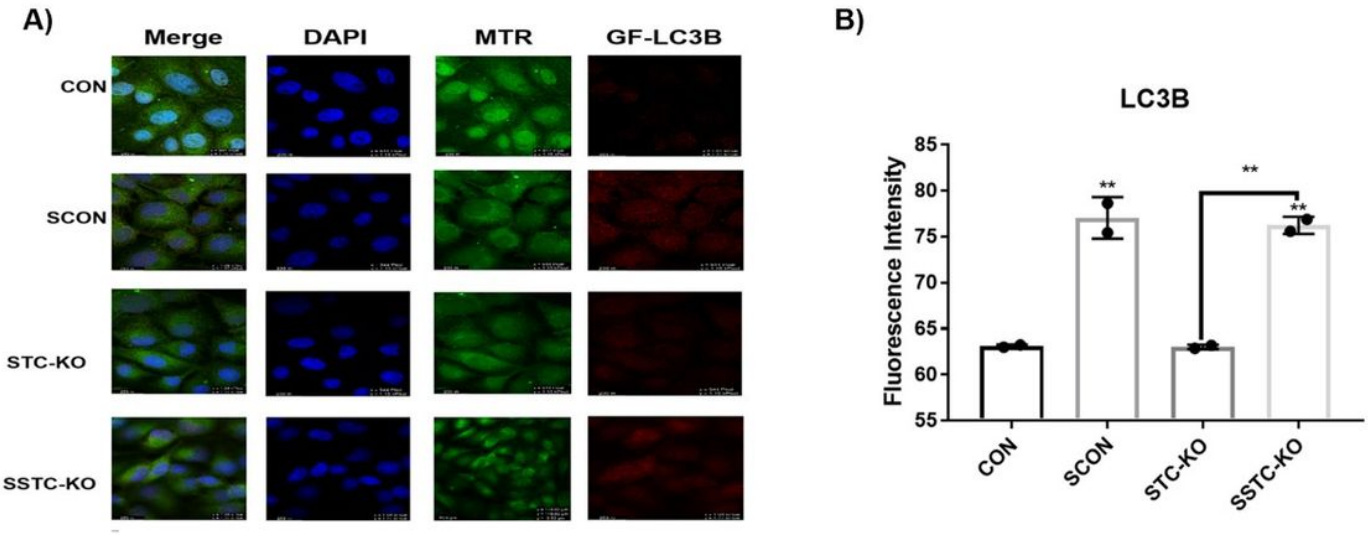

Figure 11

A) The cells were stained with immunofluorescent anti-GFP-LC3B antibody, and DAPI staining was used for nucleus localization. Green shows the intracellular mitochondria excited at 579 nm. B) Quantitative fluorescence value. Scale: 35.6 μm. Statistical comparisons were made with two-tailed Student's t tests, and one-way ANOVA. The data are presented as the means ± s.d. (n=3). Changes were considered statistically significant when P < 0.05 and P<0.01.

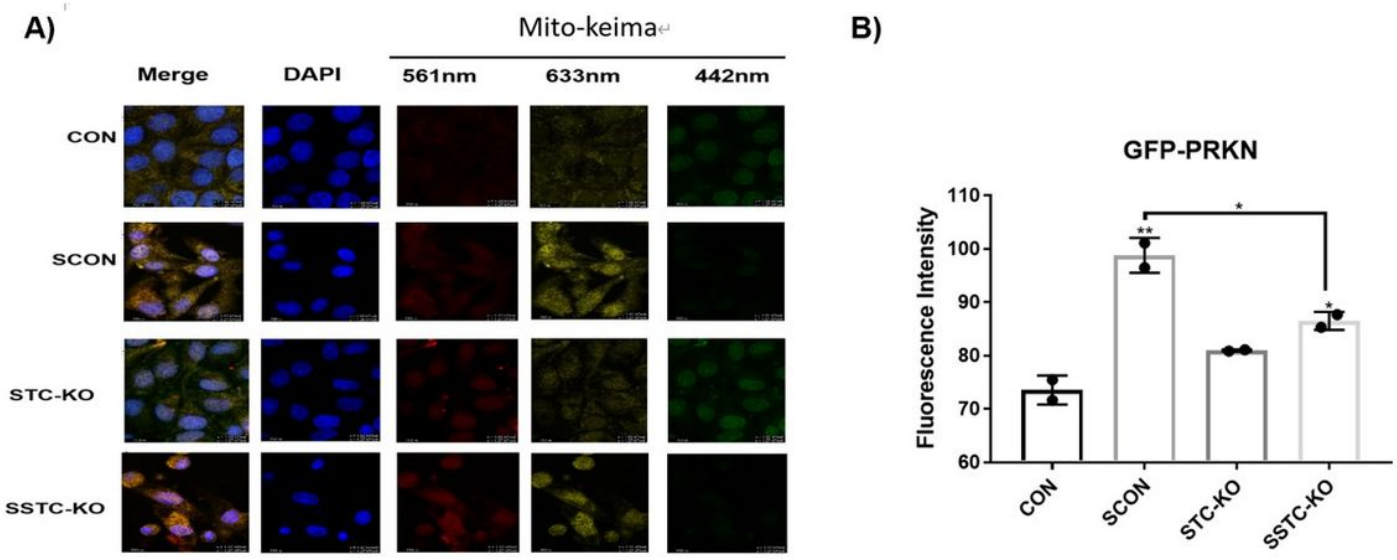

Figure 12

A) Immunofluorescence staining of cells with anti-Parkin antibody and DAPI staining for nuclear localization. Green shows intracellular mitochondria excited at 448 nm (mitochondria for measuring neutral pH), and red shows mitochondrial fluorescence when excited at 552 nm in the same cell (for acidic pH measurement). B) Quantitative fluorescence value. Scale: 35.6 μm.Statistical comparisons were made with two-tailed Student's t tests, and one-way ANOVA. The data are presented as the means ± s.d. (n=3). Changes were considered statistically significant when P < 0.05 and P<0.01.